

Chemical-Strain Induced Tilted Dirac Nodes in (BEDT-TTF)₂X₃ (X = I, Cl, Br, F) Based Charge-Transfer Salts

R. Matthias Geilhufe^{*1}, Benjamin Commeau², Gayanath W. Fernando²,

¹ Nordita, KTH Royal Institute of Technology and Stockholm University, Roslagstullsbacken 23, SE-106 91 Stockholm, Sweden

² University of Connecticut, 2152 Hillside Road, U-3046 Storrs, CT 06269-3046, USA

Key words: Dirac materials, Dirac type-II, Tilted Dirac, Charge Transfer Salts, (BEDT-TTF), Chemical Strain

* Corresponding author: e-mail geilhufe@kth.se, gayanath.fernando@uconn.edu

The identification of novel multifunctional Dirac materials has been an ongoing effort. In this connection quasi 2-dimensional (BEDT-TTF)-based charge transfer salts are widely discussed. Here, we report about the electronic structure of α -(BEDT-TTF)₂I₃ and κ -(BEDT-TTF)₂I₃ under a hypothetical substitution of iodine with the halogens bromine, chlorine and fluorine. The decreasing size of the anion layer corresponds to applying chemical strain which increases tremendously in the case of (BEDT-TTF)₂F₃. We performed structural optimization and electronic structure calculations in the framework of density functional theory, incorporating, first, the recently developed strongly constrained and appropriately normed semilocal density functional SCAN, and, second, van der Waals corrections to the PBE exchange correlation functional by means of the dDsC dispersion correction method. In the case of α -(BEDT-TTF)₂F₃ the formation of over-tilted Dirac-type-II nodes within the quasi 2-dimensional Brillouin zone can be found. For κ -(BEDT-TTF)₂F₃, the recently reported topological transition within the electronic band structure cannot be revealed.

1 Introduction Organic charge transfer salts, especially quasi two-dimensional (BEDT-TTF)₂X₃ where X represent a variety of acceptor molecules, have generated great interest over the past few decades. Depending on the structural phase, the acceptor molecules, and other factors, these can be associated with a rich variety of physical phenomena such as charge ordering, metal-insulator transitions, unconventional superconductivity, antiferromagnetism and spin liquids. In these compounds, the molecular units consisting of carbon atoms (i.e., donors) usually preserve their specific features and are separated by layers of anion atoms that act as acceptors. It is believed that the unpaired electrons (or holes) in the carbon π -orbitals are responsible for the conducting properties.

The α -phase with X=I represents a narrow band-gap semiconductor at ambient pressure [1] showing charge ordering as investigated by synchrotron X-ray diffraction measurements [2]. Under high pressure, it was reported that α -(BEDT-TTF)₂I₃ exhibits a transition to a semi-metallic phase exhibiting tilted Dirac-crossings within the

band structure [3,4,5,6,7,8,9]. Although Dirac materials have been of major interest recently [10], α -(BEDT-TTF)₂I₃ under high pressure is one of the few non-planar organic Dirac materials known to date [11, 12]. In general, organic compounds satisfying specific filling-constraints [13] favorable for exhibiting a semimetallic phase tend to be susceptible to interaction instabilities which break the global symmetry of the system and with that eliminate the protection of the semi-metallic phase [14]. However, for sufficiently high temperatures, above the transition temperature of the instability, and incorporating chemical strain we argue that the quasi 2-dimensional material α -(BEDT-TTF)₂F₃ is likely to host heavily tilted Dirac-cones at ambient pressure.

We have recently reported first principles-based band structure calculations for α - and β -phases with X=I and κ -phase with X=I, Br, Cl and F [15]. For the latter it was found that the isovalent replacements of Iodine with Bromine, Chlorine and Fluorine leads to a chemical-strain induced topological band crossing along the path Γ -Y

within the Brillouin zone, which is protected by the non-symmorphic symmetry present for the κ -phase.

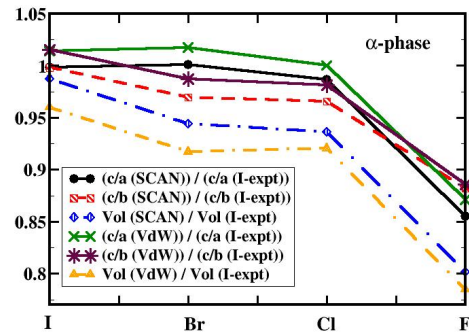
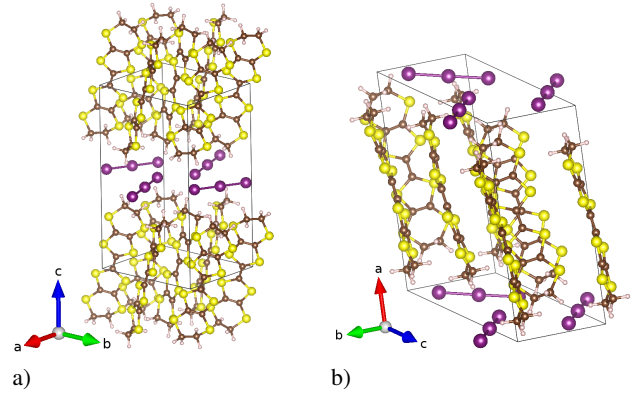
In the present work, we complement the previous study by revising and extending this discussion for the κ - and α -phases incorporating very recently developed exchange correlation functionals within the framework of the density functional theory (DFT). Here, α -(BEDT-TTF) $_2$ X $_3$ is found to be of particular interest, due to emerging tilted (and over-tilted) Dirac crossings within the band structure. Furthermore, we rigorously discuss the structural changes and charge transfer connected to the incorporated chemical strain. We point out that the chemically induced strains may not necessarily be similar to those due to hydrostatic pressure. Although the numerical values of charge transfer may depend on the selected appropriation scheme, the trends in charge transfer yield useful and consistent insights into the donor-acceptor nature of various atoms based on the DFT framework.

The paper is structured as follows. First, we discuss the change of the cell volume by inducing chemical strain mediated by the substitution of the iodine layer by bromine, chlorine and fluorine. Second, we report about the changing charge transfer observed by the chemical substitution. Afterwards, we discuss the change of the electronic structure for α -(BEDT-TTF) $_2$ X $_3$ and κ -(BEDT-TTF) $_2$ X $_3$ due to the decreased unit cell size.

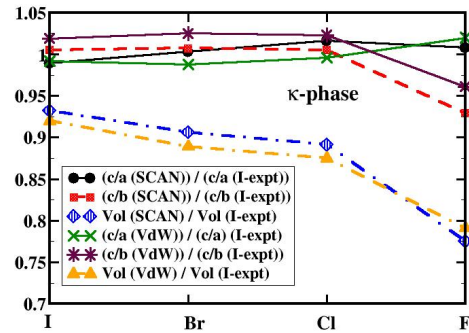
2 Volume and Lattice Parameter Ratios Under Chemical Substitution We have examined the effects of changing the anion X in α -(BEDT-TTF) $_2$ X $_3$ and κ -(BEDT-TTF) $_2$ X $_3$ in the framework of the DFT by applying a pseudopotential projector augmented-wave method [16, 17, 18, 19], as implemented in the Vienna Ab initio Simulation Package (VASP) [20, 21] and Quantum Espresso [22]. The exchange correlation functional was approximated by the recently developed semilocal meta-GGA functional (SCAN) [23, 24]. Additionally, we performed calculations in the framework of the generalized gradient approximation (PBE) [25], incorporating Van der Waals corrections in terms of the dDsC dispersion correction method (VdW) [26, 27].

The calculations were performed without spin-orbit coupling, which is a reasonable approximation due to the light elements within the (BEDT-TTF) $_2$ I $_3$ molecule. For the integration in k -space, a $6 \times 6 \times 6$ Γ -centered mesh according to Monkhorst and Pack [28] was chosen during the self-consistent cycle. The precision flag was set to “normal”. A structural optimization was performed by allowing the ionic positions, the cell shape, and the cell volume to change (ISIF = 3).

Quantum ESPRESSO was applied to estimate the associated irreducible representations of the energy levels within the band structure. The cut-off energy for the wave function was chosen to be 48 Ry and the cut-off energy for the charge density and the potentials was chosen to be 316 Ry. The charge transfer for the κ -phase was computed



c)



d)

Figure 1 The crystal structures with the respective a -, b -, and c -axes are shown in (a) for α -(BEDT-TTF) $_2$ X $_3$ and (b) for κ -(BEDT-TTF) $_2$ X $_3$. Volume, c/a , and c/b ratio changes under chemical substitution I \rightarrow Br, Cl, Fr (c) α -(BEDT-TTF) $_2$ X $_3$ and (d) κ -(BEDT-TTF) $_2$ X $_3$.

using projected wavefunctions onto orthogonalized atomic wavefunctions, which calculates the Lowdin charges.

The basic structural parameters of α -(BEDT-TTF) $_2$ I $_3$ and κ -(BEDT-TTF) $_2$ I $_3$ were taken from the Cambridge Structural Database (CSD) [29,30,31]. An illustration of the molecular ordering as well as the chosen unit cells for α -(BEDT-TTF) $_2$ X $_3$ and κ -(BEDT-TTF) $_2$ X $_3$ is shown in Figure 1 (a), (b). The (BEDT-TTF) layers and the anion layer are stacked alternately in these materials and the latter is thought to be insulating. The bands near the Fermi level are mostly originating from (BEDT-TTF) layers, with the main contributions originating from the C and S p -orbitals [15]. In the κ -phase, there is a set of bonding (occupied) and antibonding (partially occupied) bands in the vicinity of the Fermi level. We have examined the role of the anion layer as follows. The α - and κ -phases of (BEDT-TTF) $_2$ I $_3$ were studied by replacing all the iodine atoms with another halogen atom, namely bromine, chlorine, and fluorine. These atoms are isovalent and smaller in size compared to iodine and hence can induce “chemical strains”, giving rise to a compression of the original unit cell.

We have monitored the relaxed volumes of the unit cell under such substitutions and found a steady decrease in the volume of the unit cell under the progressive substitutions I \rightarrow Br \rightarrow Cl \rightarrow F. Figures 1 (c) and (d) show the relative change of the unit cell volume and c/a and c/b ratios with respect to the experimentally observed values [30,31] for α -(BEDT-TTF) $_2$ I $_3$ and κ -(BEDT-TTF) $_2$ I $_3$. In the α -phase, under the above progressive substitution, c/a and c/b ratios also show an almost steady decrease. In this case, the c -axis is the long axis of the crystal, while \hat{a} and \hat{b} vectors span a plane almost perpendicular to the c -axis. The steady decrease of the c/a and c/b ratios is due to a relatively large contraction along the c axis compared to somewhat smaller changes in the plane spanned by \hat{a} and \hat{b} vectors. This change can be directly attributed to the decrease of the atom size in the insulating (acceptor) layers under the substitution I \rightarrow Br \rightarrow Cl \rightarrow F. The induced chemical strain may be designated as an almost uniaxial strain. The analogous changes in the κ -phase look more subtle. Note here that the long axis in this case is the a -axis while the b -axis is the special axis in this monoclinic structure (which is perpendicular to both a - and c -axes), according to our choice of axes shown in Fig. 1 (d). Note that the c/a ratio remains steady during the above progressive substitution although both a and c parameters decrease. Also noteworthy is the fact that the parameter b does not show changes comparable to those associated with c and a . This case may be interpreted as indicating a biaxial strain. The results are consistent for both exchange correlation functionals SCAN and VdW corrected PBE. For the α -(BEDT-TTF) $_2$ I $_3$, the structural information obtained incorporating the SCAN functional is in almost perfect agreement with the experimental values, whereas the cell volume is underestimated by about 5 % using the VdW method. However, both functionals underestimate the cell volume for κ -(BEDT-TTF) $_2$ I $_3$ by about 7% for SCAN and 8% for VdW.

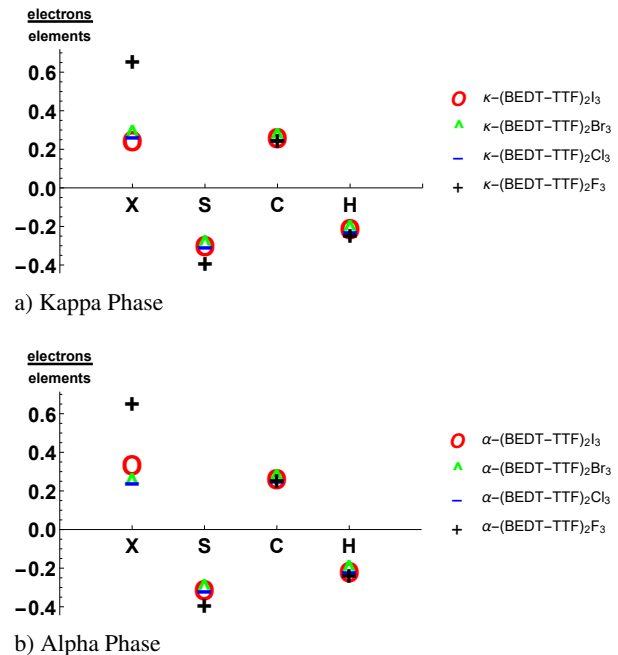


Figure 2 Charge transfer under chemical substitution for the halogen atoms (X=I,Br,Cl,F). The charge transfer is the net electron charge displaced with respect to the atom’s valence electrons averaged over all atoms of the same element type. The valence electron numbers of each atom are (7,6,4,1) for (I,S,C,H) respectively. For example, κ -(BEDT-TTF) $_2$ F $_3$ gained an additional 0.65 electron charge to each of its six fluorine atoms on average, giving it a total average of 7.65 electron charge to its valence electrons.

3 Charge Transfer Figure 2a and 2b illustrate the charge transfer for α -(BEDT-TTF) $_2$ X $_3$ and κ -(BEDT-TTF) $_2$ X $_3$, respectively. Both sets of data have consistent charge transfer behavior. Charge is transferred from the sulfur and hydrogen atoms to the carbon and halogen atoms. Fluorine gains twice as much charge compared to the other halogens.

Figure 3a illustrates a gradual movement of the halogens I \rightarrow Br \rightarrow Cl under chemical substitution ion relaxation in the kappa phase, and a large displacement in the location of 3 of its fluorine atoms. To our knowledge, there are no publications related to the synthesis of (BEDT-TTF) $_2$ F $_3$. Fluorine, as a single atom, has shown in our relaxation calculations to be very electronegative and attempts to form strong charge transfer bonds with the other atoms in the crystal. However, we note here that organic crystals with an isolated anion fluorine atom can be synthesized in general[32].

4 Symmorphic α -phase The α -phases of (BEDT-TTF) $_2$ X $_3$ crystallize in a triclinic crystal structure, having the (symmorphic) space group $P\bar{1}$ (#2). Under ambient pressure, α -(BEDT-TTF) $_2$ I $_3$ is a narrow band-gap insula-

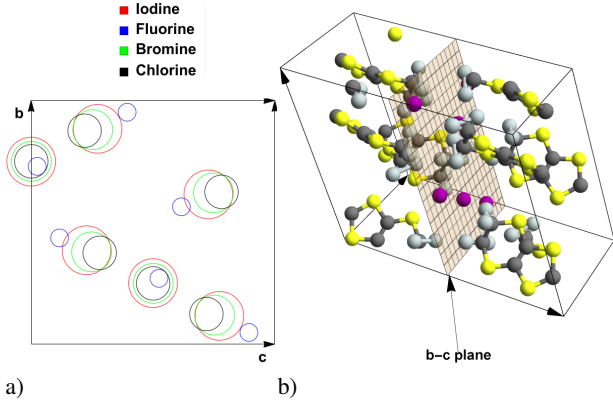
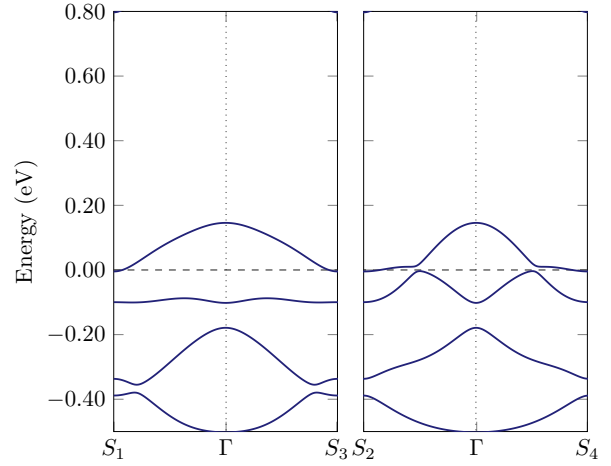


Figure 3 Halogen movement under chemical substitution for κ -(BEDT-TTF) $_2$ X $_3$ for X=(I,Br,Cl,F) in the b - c -plane, spanned by lattice vectors b and c . (a) Top down view of normalized b - c -plane (lattice vectors normalized to equal length). Circles' centers are the halogen locations for κ -(BEDT-TTF) $_2$ X $_3$ for X=(I,Br,Cl,F). (b) b - c -plane cut where halogens (purple atoms) exist in 3D crystal unit cell for κ -(BEDT-TTF) $_2$ X $_3$.

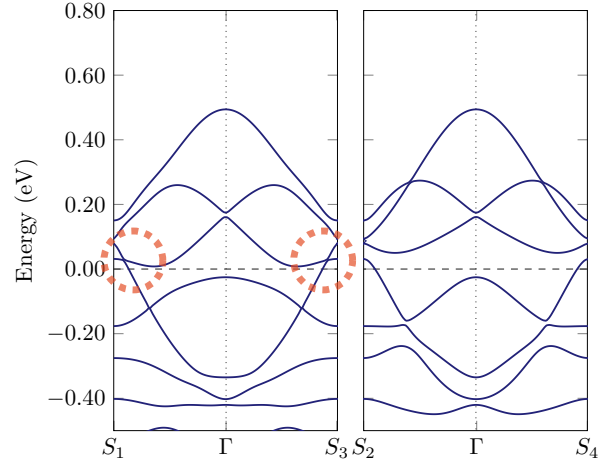
tor as shown in Figure 4a. The “tilted Dirac cone” reported in α -(BEDT-TTF) $_2$ I $_3$ under high pressure is centered at an interior k -point in the Brillouin zone [3, 4, 5, 6, 7, 8, 9]. The placement of the Dirac point in k -space is similar to what is observed in strained graphene where the Dirac points in unstrained graphene get dragged away from the high symmetry K and K' points. The “tilt parameter” in this case has been shown to depend linearly on the strain [33]. The linear (and tilted) bands, if placed near the Fermi level, can give rise to distinct transport properties.

The substitution of I with Br and Cl, does not change the band structure qualitatively. However, the decreasing unit cell size lowers the energy of several high-lying bands and additionally decreases the band gap along the path $S_2 - \Gamma - S_4$. Interestingly, the situation dramatically changes for a substitution $I \rightarrow F$, leading to a huge increase of the band gap along $S_2 - \Gamma - S_3$ and over-tilted band crossings along $S_1 - \Gamma - S_3$, as can be seen in Fig. 4b. As each band additionally carries a spin-degeneracy, the total degeneracy at the crossing points is four. Such materials are referred to as Dirac type-II semimetals. The same tilted crossings are revealed incorporating the PBE functional and Van der Waals corrections.

Recently, Dirac type-II and Weyl type-II materials have attracted a lot of attention, as they are discussed to effectively mimic the behavior of Dirac or Weyl fermions in the vicinity of a strong gravitational field [34, 35, 36, 37]. The influence of the effective gravitational field leads to a curved metric and a tilted light or Dirac cone in the case of massless fermions. In this picture, an over-tilted Dirac-cone refers to Fermions beyond the event-horizon of a black hole, where the particle momentum is com-



a)



b)

Figure 4 Band structure of (a) α -(BEDT-TTF) $_2$ I $_3$ and (b) α -(BEDT-TTF) $_2$ F $_3$ calculated using VASP and the SCAN meta-GGA functional. The high symmetry points represent the corners of the quasi-2D Brillouin zone given by $S_1 = (0.5, 0.5, 0.0)$, $S_2 = (0.5, -0.5, 0.0)$, $S_3 = (-0.5, 0.5, 0.0)$, and $S_4 = (-0.5, -0.5, 0.0)$.

pletely suppressed away from the origin of the gravitational field. Thus, the investigation of materials like α -(BEDT-TTF) $_2$ F $_3$ with effective excitations given by Dirac type-II fermions can lead to important insights of black hole physics by means of condensed matter systems.

5 Nonsymmorphic κ phase The κ -phase crystallizes in a monoclinic crystal structure having the space group $G \equiv P12_11$ (#4), which can be represented by the coset decomposition

$$G = \mathcal{T} \cup (\{C_{2y}|(0, 1/2, 0)\} \odot \mathcal{T}). \quad (1)$$

Here, $\{C_{2y}|(0, 1/2, 0)\}$ denotes a two-fold screw symmetry, represented by a two-fold rotation about the y -axis together with a non-primitive shift along the lattice vector \mathbf{a}_2 . The nonsymmorphic nature of the space group leads to degenerate line-nodes along the Brillouin zone boundary. Nonsymmorphic symmetries were widely discussed in protecting Dirac nodes [38,39,40,41]. In general, it is possible to distinguish between crossings protected by the crystalline symmetry, i.e., crossings which are associated with higher dimensional irreducible representations or pairs of complex-conjugate irreducible representations, and crossings protected by band topology, where the bands belong to different irreducible representations (accidental crossings), but where the crossing is forced to occur due to the connectivity of the bands [11, 12, 42, 43, 44].

The band structure of κ -(BEDT-TTF) $_2$ I $_3$ close to the Fermi level is shown in Fig. 5a. Within the energy range of $[-0.8, 0.4]$ two pairs of two bands can clearly be revealed. Here, the bands occur pair-wise as the nonsymmorphic symmetry protects the degeneracy at the Brillouin zone boundary. As discussed in [15], each pair consists of one band transforming even (irrep A at the Γ -point) and one band transforming odd (irrep B at the Γ -point) under C_{2y} . Here, the four bands illustrated in Fig. 5a correspond to an ordering of A, B, A, B , from the lowest to the highest band. However, in Ref. [15] it was reported that a substitution of $I \rightarrow F$ leads to a shift upwards of the bands, and, in addition to that, to a change of the ordering of the levels at the Γ point to A, A, B, B . This ordering introduces a topologically protected crossing along the path $\Gamma - Y$. However, the present calculations performed using the SCAN functional do not support this change of the ordering, but reveal a band touching along $\Gamma - Y$ (see Fig. 5b). A similar behavior is also found for the calculations performed using the VdW-corrected PBE functional.

6 Universal Phase Diagrams Universal phase diagrams summarizing the rich physics of the α and κ -phases have been presented following the work of Refs. [45, 46]. The κ -phase diagram, which was published first in Ref. [45] for (BEDT-TTF) $_2$ Y where Y=Cu(NCS) $_2$ combined with selected halogens, has been compared to the well-known (and strongly correlated) V $_2$ O $_3$ phase diagram. It was noted there that, for this phase, the chemical pressure and the strength of correlations act in the opposite direction to the hydrostatic pressure. To our knowledge, the BEDT-TTF compound corresponding to fluorine substitution has not been synthesized. If it can be synthesized, its placement in such a phase diagram will be quite interesting. This is due to our calculated results which show a behavior somewhat different from the trends seen for Cl and Br substitutions. In the latter cases, the changes in the electronic and lattice structures are gradual and predictable. However, the changes in the lattice constant ratios as well as volume are relatively significant under fluorine substitution. The induced chemical strains are not

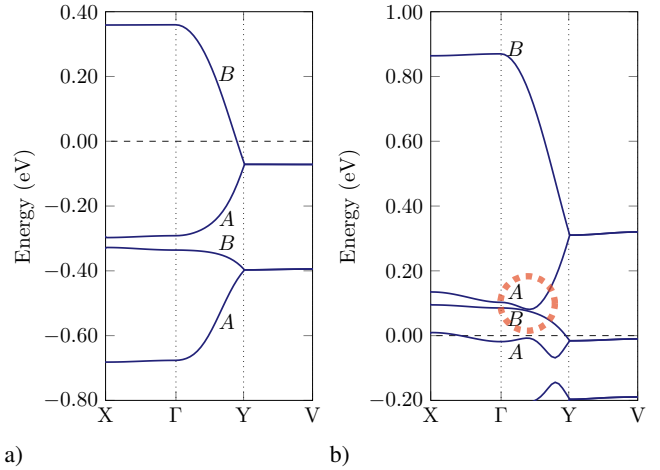


Figure 5 Band structure of (a) κ -(BEDT-TTF) $_2$ I $_3$ and (b) κ -(BEDT-TTF) $_2$ F $_3$ calculated using VASP and the SCAN meta-GGA functional. The high symmetry points are $X = (0.5, 0.0, 0.0)$, $Y = (0.0, 0.5, 0.0)$, and $V = (0.5, 0.5, 0.0)$.

necessarily isotropic and may not resemble those due to hydrostatic pressure. The phase diagram indicates that the fluorine compound is likely to lead to equally or more rich physical properties, if it can be synthesized. However, any other small set of atoms as the insulating layers (even though not chemically similar) may give rise to fascinating physical properties.

7 Conclusions Organic materials based on (BEDT-TTF) $_2$ X $_3$ (X=I, Br, Cl, F) show great potential for fine tuning specific band structures near the Fermi level due to their softness. Our research shows that applying chemical strain to the α - and κ - phases creates significant changes in the volume and ratios of their lattice constants. From the structural optimization it follows that the mutual replacement of iodine with bromine, chlorine and fluorine corresponds to an almost uniaxial strain applied to the sample. The structural optimization also give insights into the accuracy of the recently developed exchange-correlation functionals SCAN and VdW-corrected PBE. For SCAN we find a very good agreement with the experimental unit cell for α -(BEDT-TTF) $_2$ I $_3$. However, for the κ -phase, both functionals underestimate the cell volume. As a result of the chemical strain, we observe over-tilted Dirac-type-nodes in the α -phase for α -(BEDT-TTF) $_2$ F $_3$. These crossings exhibit a four-fold degeneracy. For the nonsymmorphic κ -phase, the existence of a topological transition has been examined and questioned throughout this work. This research highlights the promise and importance of tuning the band structure using chemical or other strains that could lead to creating multi-functional Dirac materials. Additionally, our calcu-

lations can be used as a starting point to probe strong correlations known to exist in such compounds.

8 Acknowledgement We thank Dr. A. V. Balatsky for his support and helpful discussions concerning this study. We are grateful for support from the Swedish Research Council Grant No. 638-2013-9243, the Knut and Alice Wallenberg Foundation, and the European Research Council under the European Union’s Seventh Framework Program (FP/2207-2013)/ERC Grant Agreement No. DM-321031. The authors acknowledge computational resources from the Swedish National Infrastructure for Computing (SNIC) at the High Performance Computing Center North (HPC2N), the High Performance Computing (HPC) cluster at the University of Connecticut, and the computing resources provided by the Center for Functional Nanomaterials, which is a U.S. DOE Office of Science Facility, at Brookhaven National Laboratory under Contract No. de-sc0012704.

References

- [1] N. Tajima, S. Sugawara, M. Tamura, Y. Nishio, and K. Kajita, *Journal of the Physical Society of Japan* **75**(5), 051010–051010 (2006).
- [2] T. Kakiuchi, Y. Wakabayashi, H. Sawa, T. Takahashi, and T. Nakamura, *Journal of the Physical Society of Japan* **76**(11), 113702–113702 (2007).
- [3] D. Liu, K. Ishikawa, R. Takehara, K. Miyagawa, M. Tamura, and K. Kanoda, *Physical Review Letters* **116**(22), 226401 (2016).
- [4] M. Hirata, K. Ishikawa, K. Miyagawa, M. Tamura, C. Berthier, D. Basko, A. Kobayashi, G. Matsuno, and K. Kanoda, *Nature Communications* **7**, 12666 (2016).
- [5] K. Kajita, Y. Nishio, N. Tajima, Y. Suzumura, and A. Kobayashi, *Journal of the Physical Society of Japan* **83**(7), 072002 (2014).
- [6] T. Morinari and Y. Suzumura, *Journal of the Physical Society of Japan* **83**(9), 094701 (2014).
- [7] K. Miyahara, M. Tsuchiizu, and A. Kobayashi, A possible massless dirac electron in molecular two-orbital model, in: *Proceedings of the International Conference on Strongly Correlated Electron Systems (SCES2013)*, (2014), , 017011.
- [8] R. Kondo, S. Kagoshima, N. Tajima, and R. Kato, *Journal of the Physical Society of Japan* **78**(11), 114714 (2009).
- [9] T. Mori, *Journal of the Physical Society of Japan* **79**(1), 014703 (2009).
- [10] T. Wehling, A. M. Black-Schaffer, and A. V. Balatsky, *Advances in Physics* **63**(1), 1–76 (2014).
- [11] R. M. Geilhufe, A. Bouhon, S. S. Borysov, and A. V. Balatsky, *Physical Review B* **95**(4), 041103 (2017).
- [12] R. M. Geilhufe, S. S. Borysov, A. Bouhon, and A. V. Balatsky, *Scientific Reports* **7** (2017).
- [13] H. Watanabe, H. C. Po, M. P. Zaletel, and A. Vishwanath, *Physical review letters* **117**(9), 096404 (2016).
- [14] B. Wieder, R. M. Geilhufe, S. S. Borysov, and A. V. Balatsky, submitted.
- [15] B. Commeau, R. M. Geilhufe, G. W. Fernando, and A. V. Balatsky, *Physical Review B* **96**, 125135 (2017).
- [16] D. Hamann, M. Schlüter, and C. Chiang, *Physical Review Letters* **43**(20), 1494 (1979).
- [17] P. E. Blöchl, *Physical Review B* **50**(24), 17953 (1994).
- [18] D. Vanderbilt, *Physical Review B* **41**(11), 7892 (1990).
- [19] G. Kresse and J. Hafner, *Journal of Physics: Condensed Matter* **6**(40), 8245 (1994).
- [20] G. Kresse and J. Furthmüller, *Physical Review B* **54**(16), 11169 (1996).
- [21] G. Kresse and D. Joubert, *Physical Review B* **59**(3), 1758 (1999).
- [22] P. Giannozzi, S. Baroni, N. Bonini, M. Calandra, R. Car, C. Cavazzoni, D. Ceresoli, G. L. Chiarotti, M. Cococcioni, I. Dabo, A. D. Corso, S. de Gironcoli, S. Fabris, G. Fratesi, R. Gebauer, U. Gerstmann, C. Gougoussis, A. Kokalj, M. Lazzeri, L. Martin-Samos, N. Marzari, F. Mauri, R. Mazzarello, S. Paolini, A. Pasquarello, L. Paulatto, C. Sbraccia, S. Scandolo, G. Sclauzero, A. P. Seitsonen, A. Smogunov, P. Umari, and R. M. Wentzcovitch, *Journal of Physics: Condensed Matter* **21**(39), 395502 (2009).
- [23] J. Sun, A. Ruzsinszky, and J. P. Perdew, *Physical Review Letters* **115**(Jul), 036402 (2015).
- [24] J. Sun, R. C. Remsing, Y. Zhang, Z. Sun, A. Ruzsinszky, H. Peng, Z. Yang, A. Paul, U. Waghmare, X. Wu et al., *Nature chemistry* **8**(9), 831 (2016).
- [25] J. P. Perdew, K. Burke, and M. Ernzerhof, *Physical review letters* **77**(18), 3865 (1996).
- [26] S. N. Steinmann and C. Corminboeuf, *Journal of Chemical Theory and Computation* **7**(11), 3567–3577 (2011).
- [27] S. N. Steinmann and C. Corminboeuf, *The Journal of chemical physics* **134**(4), 044117 (2011).
- [28] H. J. Monkhorst and J. D. Pack, *Physical Review B* **13**(12), 5188 (1976).
- [29] C. R. Groom, I. J. Bruno, M. P. Lightfoot, and S. C. Ward, *Acta Crystallographica Section B* **72**(2), 171–179 (2016).
- [30] H. Endres, H. J. Keller, R. Swietlik, D. Schweitzer, K. Angermund, and C. Krüger, *Zeitschrift für Naturforschung A* **41**(11), 1319–1324 (1986).
- [31] A. Kobayashi, R. Kato, H. Kobayashi, S. Moriyama, Y. Nishio, K. Kajita, and W. Sasaki, *Chemistry Letters* **16**(3), 459–462 (1987).
- [32] J. Touret, X. Bourdon, M. Leblanc, R. Retoux, J. Renaudin, and V. Maisonneuve, *Journal of Fluorine Chemistry* **110**(2), 133–138 (2001).
- [33] M. O. Goerbig, J. N. Fuchs, F. Piechon, and G. Montambaux, *Physical Review B* **78**, 045415 (2008).
- [34] G. G. Pyrialakos, N. S. Nye, N. V. Kantartzis, and D. N. Christodoulides, *Physical Review Letters* **119**(Sep), 113901 (2017).
- [35] M. Trescher, B. Sbierski, P. W. Brouwer, and E. J. Bergholtz, *Physical Review B* **95**(Jan), 045139 (2017).
- [36] A. A. Soluyanov, D. Gresch, Z. Wang, Q. Wu, M. Troyer, X. Dai, and B. A. Bernevig, *Nature* **527**(7579), 495 (2015).
- [37] G. E. Volovik, *JETP letters* **104**(9), 645–648 (2016).
- [38] L. M. Schoop, M. N. Ali, C. Straßer, A. Topp, A. Varykhalov, D. Marchenko, V. Duppel, S. S. Parkin, B. V. Lotsch, and C. R. Ast, *Nature communications* **7** (2016).

-
- [39] B. J. Wieder, Y. Kim, A. Rappe, and C. Kane, Physical review letters **116**(18), 186402 (2016).
- [40] S. M. Young, S. Zaheer, J. C. Teo, C. L. Kane, E. J. Mele, and A. M. Rappe, Physical review letters **108**(14), 140405 (2012).
- [41] Y. Chen, H. S. Kim, and H. Y. Kee, Physical Review B **93**(15), 155140 (2016).
- [42] B. J. Wieder and C. L. Kane, Physical Review B **94**(Oct), 155108 (2016).
- [43] A. Bouhon and A. M. Black-Schaffer, Physical Review B **95**(Jun), 241101 (2017).
- [44] B. Bradlyn, L. Elcoro, J. Cano, M. Vergniory, Z. Wang, C. Felser, M. Aroyo, and B. A. Bernevig, Nature **547**, 298–305 (2017).
- [45] K. Kanoda, Hyperfine Interactions **104**, 235–249 (1997).
- [46] T. Mori, H. Mori, and S. Tanaka, Bull. Chem. Soc. Jpn **72**, 179–197 (1999).